Transition from single-molecule to cooperative dynamics in a simple glass former: Raman line-shape analysis

N. V. Surovtsev, S. V. Adichtchev, and V. K. Malinovsky
Institute of Automation and Electrometry, Russian Academy of Sciences, Novosibirsk, 630090, Russia
(Received 23 April 2007; published 14 August 2007)

Parameters for orientational and inhomogeneous broadening are found from the line shape analysis of the Raman spectrum of the glass former α-picoline during cooling from low-viscous to glassy state. The orientational phase loss time τ_{OPL}, extracted from the analysis, coincides with the α relaxation time at $T>T_A$, where T_A is the temperature of transition from an Arrhenius-like to a non-Arrhenius behavior for the α-relaxation time dependence on temperature. At lower temperatures $\tau_{\mathrm{OPL}}(T)$ continues the Arrhenius behavior, in contrast to the α-relaxation time. The width of inhomogeneous broadening of the Raman line decreases noticeably as temperature increases in the temperature range $T_g<T<T_A$, approaching to zero at $T\sim T_A$. The findings evidence the transition of molecular dynamics from individual to cooperative at $T=T_A$.

DOI: 10.1103/PhysRevE.76.021502 PACS number(s): 64.70.Pf, 33.20.Fb, 61.43.Fs

The understanding of vitrification is a very interesting topic in condensed matter physics, and numerous theoretical and experimental efforts are applied to solve this problem [1–4]. Probably, one of the most important aspects of vitrification is the transition from predominantly single-molecule relaxation dynamics to cooperative dynamics. Indeed, a single-molecule description is expected to be adequate for molecular dynamics of a liquid substance in the high-temperature, low-viscous regime. On the other hand, the relaxation dynamics near the glass transition temperature T_g, is known to be highly cooperative and to involve few or many molecules. In this temperature range the structural α-relaxation function is usually nonexponential and the temperature dependence of the α-relaxation time has a non-Arrhenius behavior [1–4]. How do we experimentally quantify the transition from single-molecule to cooperative dynamics? How sharp is this transition? In this article we show that the Raman shape analysis is capable of revealing the transition, and two very astonishing outcomes are found from this analysis.

It is known that the Raman line can be considered as a composition of two spectra: anisotropic and isotropic. Experimentally, the anisotropic spectrum corresponds to scattering with the polarization change I_{HV} and the isotropic spectrum I_{iso} is a combination of I_{HV} and I_{VV}, corresponding to scattering without a change in polarization [5],

$$I_{\mathrm{iso}}(\nu) = I_{VV}(\nu) - 4/3 I_{HV}(\nu). \tag{1}$$

As the rotational motion of a molecule has a projection only to the anisotropic spectrum, the anisotropic spectrum is the convolution of the isotropic spectrum and the orientational relaxation response [5]. The orientational relaxation time τ_{OPL}, corresponding to the orientational phase loss of the molecule vibration, can be estimated from the difference in the full widths at half maximum (FWHM) of the anisotropic spectrum γ_{ani} and of the isotropic spectrum γ_{iso} [5]

$$\tau_{\mathrm{OPL}}^{-1} = \pi c(\gamma_{\mathrm{ani}} - \gamma_{\mathrm{iso}}). \tag{2}$$

Equation (2) implies that the broadening of the line is caused by relaxation. In this case the Raman line shape is a Lorentz contour

$$I(\nu) \propto \frac{1}{1 + 4(\nu - \nu_0)^2/\gamma^2}, \tag{3}$$

where ν_0 marks the line center position and γ corresponds to the linewidth. In the case of I_{iso} the line width γ_{iso} includes all relaxation and/or dissipation processes except the orientation relaxation. The line shape of I_{ani} includes the orientational relaxation. Since, the convolution of two Lorentz contours is again a Lorentz contour with the width being the sum of widths of initial contours, then the linewidth γ_{ani} is the sum of γ_{iso} and the linewidth of the Lorentz contour, corresponding to the orientational relaxation (2). The linewidth found from an experimental data includes also inhomogeneous and instrumental broadening. If this broadening does not exceed significantly the relaxation linewidth then it can be considered as an additive correction to an experimental γ. Since with a good expected precision this correction is the same for both anisotropic and isotropic spectra, the inhomogeneous and instrumental broadening is subtracted in Eq. (2) and have no effect on τ_{OPL}^{-1} found from Eq. (2). One notable consequence of this assumption is that the instrumental resolution itself does not distort τ_{OPL}^{-1}. The precision of this assumption in our experiment will be demonstrated below.

The orientational relaxation time found via Eq. (2) has some different meanings, as compared to conventional relaxation time probing by other experimental methods. First, this orientational time is attributed to single-molecule dynamics. (An exchange by orientations between two molecules is a relaxation act in this case, in contrast to, for example, dielectric spectroscopy, where this exchange does not contribute to the signal.) Second, τ_{OPL} reflects the rate of how quickly the wave function describing the orientation state of a molecule loses its phase memory. In a certain sense, τ_{OPL} corresponds to "attempts" of a molecule to change the orientation rather than the reorientation realization. The knowledge of $\tau_{\mathrm{OPL}}(T)$ and its interrelation with the behavior of the α-relaxation time τ_α would help in understanding how the cooperative dynamics emerges from the single-molecule dynamics.

 ©2007 The American Physical Society

In the present work we revive early investigations of τ_{OPL}, taking advantage of modern multichannel spectrometers, which allow us to measure Raman spectra with a much better defined spectral shape. So, it is possible now to extract narrower orientational broadening of a line and to distinguish the inhomogeneous broadening from the relaxation broadening.

We have studied the molecular glass former α picoline (T_g=133 K), which was investigated by other experimental methods up to 320 K [6]. To extend the temperature range of $\tau_\alpha(T)$, the low-frequency Raman scattering of α-picoline was measured at T=333, 353, 373, and 393 K (a laser line of 633 nm, TriVista 777 spectrometer in subtractive mode, spectra were recorded down to 1 cm^{-1} with resolution of 0.5 cm^{-1}). In studying orientational broadening, Raman lines with the depolarization ratio in the range 0.1–0.5 are preferable, since lower or higher depolarization ratios provoke difficulties with I_{ani} or I_{iso} extraction in experiments. Lines near 548 and 629 cm^{-1} of the α-picoline Raman spectrum are well suitable for the study (depolarization ratios of 0.2 and 0.4, respectively). Characteristic assignment of these lines is CCC and CNC bending [7]. Hence, the orientation motion revealed by Eq. (2) is expected to reflect the motion of a molecule as whole. Results obtained for these lines agree with each other; for the rest of our paper the main outcomes will be illustrated by results for the 548 cm^{-1} line.

Two series of experiments were performed with a triple grating TriVista 777 spectrometer, equipped by a multichannel CCD-camera. In the first series, a line of 532 nm from a solid-state laser was used, and the spectral resolution in the subtractive mode of the spectrometer was 1.7 cm^{-1} (FWHM), as checked by a neon-discharge lamp spectrum. In the second series, a line of 647 nm from a krypton laser was used, and the spectral resolution in the additive mode of the spectrometer was 0.3 cm^{-1} (FWHM, 0.037 cm^{-1} per pixel of the camera). Since instrumental broadening, as well as inhomogeneous broadening, makes identical contributions to γ_{iso} and to γ_{ani}, the experimental value of τ_{OPL} should be independent of the spectral resolution [5]. Two series of the experiment allowed us to crosscheck the validity of the results.

A representative spectral line shape for the 548 cm^{-1} line is shown in the inset of Fig. 1 for polarized (VV) and depolarized (HV) geometries. Orientational broadening is responsible for a remarkable difference in the spectral width for two light scattering geometries at T=320 K. The isotropic spectrum found via Eq. (1) is also shown in the inset of Fig. 1.

The simplest way to find τ_{OPL} is to fit the anisotropic and isotropic spectra by a Lorentz contour Eq. (3) and to use Eq. (2). The temperature dependence of $\tau_{\mathrm{OPL}}(T)$ found in this manner for the experimental resolution of 1.7 cm^{-1} is shown in Fig. 1 by solid triangles for the Arrhenius plot. The experimental series with the resolution of 0.3 cm^{-1} yields the same values, proving that the data are not distorted by the instrumental resolution. The α-relaxation time data of α-picoline extracted from other experimental methods are also shown in Fig. 1. It is seen that $\tau_{\mathrm{OPL}}(T)$ and the α-relaxation time are in good agreement in the temperature range where $\tau_\alpha(T)$ obeys the Arrhenius behavior, but they start to disagree in the temperature range where $\tau_\alpha(T)$ deviates from the Arrhenius law. In the low-temperature range, $\tau_{\mathrm{OPL}}(T)$ demonstrates a sub-Arrhenius behavior with approaching a limiting value. This limit corresponds to the difference between γ_{ani} and γ_{iso}, $\gamma_{\mathrm{low}}=\gamma_{\mathrm{ani}}-\gamma_{\mathrm{iso}}=0.09$ cm^{-1} (γ_{low} is about one third of the highest resolution used in the experiment and 2.5 times higher than the spectral interval per pixel).

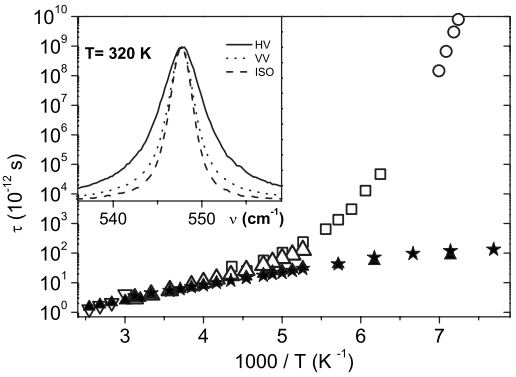

FIG. 1. Arrhenius plot for the orientational time τ_{OPL} (solid triangles and stars for the instrumental resolution of 1.7 and 0.3 cm^{-1}, respectively); the $\tau_\alpha(T)$ from light scattering data (open down and up triangles for present work and [6], respectively), neutron scattering data [8] (squares), and dielectric spectroscopy data [6] (circles). The inset shows the Raman line shape for depolarized, polarized, and isotropic spectra at T=320 K (solid, dotted, dashed lines, respectively).

This analysis can be refined by taking into account the inhomogeneous broadening. The inhomogeneous broadening is the effect of the instantaneous distribution of the molecular vibration frequency. This distribution arises from the vibration frequency shift caused by a field due to effect from neighbor molecules. In a simple assumption that the distribution of the field follows to a Gaussian distribution, the vibration frequency distribution can be described by a Gauss contour. In this case, the spectral line shape is expected to be a Voigt contour, being the convolution of the Gauss and Lorentz contours

$$I(\nu) \propto \int \frac{e^{-2(\nu_1-\nu_0)^2/\gamma_G^2}}{1+4(\nu-\nu_1)^2/\gamma_L^2} d\nu_1. \tag{4}$$

the Voigt contour includes two parameters, characterizing the linewidth γ_G and γ_L. In this case, the Gauss width γ_G corresponds to the inhomogeneous broadening and the Lorentz width γ_L corresponds to the relaxation broadening. As is illustrated in Fig. 2 for the spectral line shape at T=190 K, the experimental data reveal insufficiency of the Lorentz (or Gauss) contour, but the Voigt contour works well, and γ_G and γ_L can be found unambiguously from a single experimental spectrum. In the fitting procedure, γ_G was used as a free parameter only for the fitting isotropic spectrum (the isotropic spectrum has the smallest relaxation broadening); for fitting the anisotropic spectrum, however, γ_G was fixed at the same value as for the isotropic spectrum. Equation (2) is applied only for Lorentz's γ's, where Eq. (2) is rigorous. Voigt's analysis can be performed without ambiguity in the

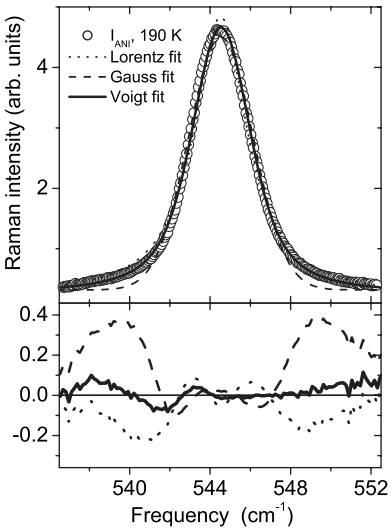

FIG. 2. Raman line in a depolarized spectrum at $T=190$ K and its fitting by Lorentz, Gauss, and Voigt contours (dotted, dashed, solid lines, respectively). The bottom part shows the relative deviation of the analytical contours from the experimental line.

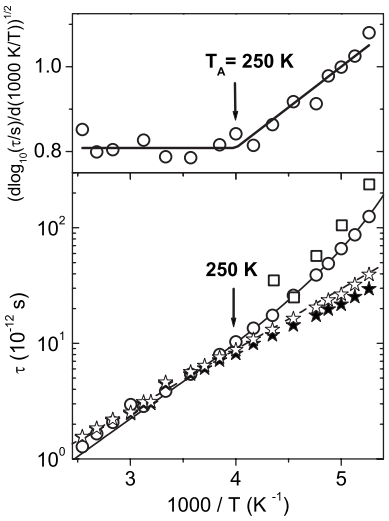

FIG. 3. Bottom part: Arrhenius plot for the orientational time τ_{OPL} noncorrected and corrected for the low-temperature limit (solid and open stars, respectively); the $\tau_\alpha(T)$ from light scattering data (circles, present work and Ref. [6]) and neutron scattering data [8] (squares); the Arrhenius behavior and the MCT fit with parameters from Ref. [6] (dashed and solid lines, respectively). Top part: the temperature dependence of $[\partial(\log_{10}\tau_\alpha)/\partial(1000/T)]^{1/2}$ versus $1000/T$ (circles), revealing the temperature T_A; the line is a description by two linear regions.

temperature range from low temperatures up to 270 K. At 280 K and higher temperatures, Voigt's analysis has no advantage in comparison with Lorentz's one (inhomogeneous broadening becomes more than fourfold smaller than relaxation broadening). If, nevertheless, we applied Voigt's analysis to experimental spectra at $T>280$ K, we found $\gamma_G \approx 0.5$ cm^{-1}, almost independent of temperature and close to the instrumental resolution. Note, also that in the temperature range below the glass transition temperature $T<T_g$ the best Voigt's fit is very close to the best Gauss contour applied to the same experimental spectrum. This result supports the assumption that the inhomogeneous broadening is well approximated by the Gauss contour.

The data for $\tau_{\mathrm{OPL}}(T)$ obtained from Voigt's analysis for the experimental resolution of 0.3 cm^{-1} are shown in Fig. 1, and good agreement between two sets of data is found. Thus, the instrumental resolution and/or inhomogeneous broadening do not distort the results of Fig. 1. A striking outcome is the disagreement between $\tau_{\mathrm{OPL}}(T)$ and $\tau_\alpha(T)$ in the temperature range where $\tau_\alpha(T)$ deviates from the Arrhenius law.

The low-temperature limit γ_{low} is explained by a difference in relaxation channels for anisotropic and isotropic part of the vibrational mode. For simplicity, this difference may be assumed to be temperature independent, and this correction can be applied for evaluating $\tau_{\mathrm{OPL}}(T)$,

$$\tau_{\mathrm{OPL}}^{-1} = \pi c(\gamma_{\mathrm{ani}} - \gamma_{\mathrm{iso}} - \gamma_{\mathrm{low}}). \quad (5)$$

The bottom part of Fig. 3 shows the thus-corrected and noncorrected $\tau_{\mathrm{OPL}}(T)$. It is seen that this correction restores the Arrhenius law for $\tau_{\mathrm{OPL}}(T)$. Thus, we conclude that $\tau_{\mathrm{OPL}}(T)$ follows the Arrhenius law in the entire temperature range presented in Fig. 3.

The dependence $\tau_{\mathrm{OPL}}(T)$ diverges from $\tau_\alpha(T)$ at $T<260\pm10$ K. This temperature can be compared with the so-called T_A temperature for α-picoline, marking the violation of the Arrhenius law. T_A value can be extracted from a derivative analysis, proposed in Ref. [9]. This analysis considers the value $[d\log_{10}\tau_\alpha/d(1/T)]^{1/2}$, which transforms the Arrhenius law into a constant and the Vogel-Fulcher-Tammann law into a linear expression versus inverse temperature [9]. The derivative analysis is presented in the top part of Fig. 3, revealing the T_A temperature about 250 K for α-picoline. The mode coupling theory (MCT) fit from Ref. [6] is plotted in Fig. 3. It is seen that T_A is also close to a high temperature ($\sim$270 K) where the MCT critical behavior starts to deviate from $\tau_\alpha(T)$.

Formally, the features of $\tau_{\mathrm{OPL}}(T)$ are similar to the expected behavior of β_{slow} relaxation [10,11]. Yet, there is some circumstance deterring the interpretation of $\tau_{\mathrm{OPL}}(T)$ as a β_{slow}-relaxation counterpart. Neat α-picoline has no detectable slow β process [6,12]. Extraction of the β_{slow}-relaxation time from a binary system [12] provides extremely great disagreement with $\tau_{\mathrm{OPL}}(T)$ (more than 6 orders of magnitude) and a 2.9 higher barrier for the Arrhenius law.

The single-molecule relaxation time $\tau_{\mathrm{SM}}(T)$ can also be studied by other experimental techniques (e.g., Ref. [13]). However, the results provided by these techniques do not show the behavior similar to that in Fig. 3, except, probably, the longitudinally detected electron spin resonance [14]. The discrepancy between the single-molecule relaxation time τ_{SM} and the α-relaxation time usually occurs at temperatures lower than T_A, where $\tau_{\mathrm{SM}}(T)$ also demonstrates a non-Arrhenius behavior [13]. In the method of [13], a molecule has to rotate really, which is constrained by its neighbors. The $\tau_{\mathrm{OPL}}(T)$ is rather related to the phase loss of the quantum wave function. Thus, τ_{OPL} is closely related to the single-molecule wave function, and can be primitively interpreted

as molecule's attempts to reorientate. It is worth noting that, in the temperature range where the cooperative behavior is important for the relaxation ($T<T_A$), the orientational wave function at short times behaves similar to single-molecule dynamics in the low-viscous state.

Since at $T>T_A$, $\tau_\alpha(T)$ and $\tau_{\mathrm{OPL}}(T)$ coincide and $\tau_{\mathrm{OPL}}(T)$ corresponds to single-particle dynamics (Fig. 3), then we can conclude that α relaxation is single-molecular-like in this temperature range. At lower temperatures the cooperative character of α-relaxation leads to non-Arrhenius behavior and to the divergence with $\tau_{\mathrm{OPL}}(T)$. Thus, the temperature T_A can be interpreted as the temperature of transition from the single-particle dynamics to a cooperative one, as temperature decreases.

The divergence between $\tau_\alpha(T)$ and $\tau_{\mathrm{OPL}}(T)$ can be compared with the divergence between the rotational and translational diffusion constants in glass-forming liquids [13,15,16]. In the last case, the divergence is often interpreted as the evidence for the onset of spatial inhomogeneity [17–20]. In this sense, the reasons for the $\tau_\alpha(T)-\tau_{\mathrm{OPL}}(T)$ divergence and for the rotational-translational divergence are similar. However, there is an important difference between two cases. The rotational-translational divergence occurs typically at T_c-MCT's critical temperature [17–20], where the relaxation time demonstrates already a non-Arrhenius behavior. In the case of the $\tau_\alpha(T)-\tau_{\mathrm{OPL}}(T)$ divergence, discussed in the present work, the divergence point is T_A, being $T_A>T_c$.

It was recently demonstrated by a computer simulation that the diffusion constant considered at short time scales exhibits an Arrhenius behavior even at low enough temperatures, where the long-time diffusion constant follows a super-Arrhenius law [21]. The data of $\tau_{\mathrm{OPL}}(T)$, Fig. 3, support the conclusion of Ref. [21]. In the spirit of Ref. [21], one can suppose that the discussed $\tau_{\mathrm{OPL}}(T)$ is more sensitive to instantaneous spatial inhomogeneities, while in the case of the translational diffusion constant the spatial inhomogeneities during a certain time are more important. Probably, the different time scales explain, why the decoupling of diffusion and relaxation is detected at much higher temperatures in simulations in comparison with experiments [19,22].

The inhomogeneous broadening width γ_G found from Voigt's analysis leads to another striking outcome, presented in Fig. 4. The parameter γ_G describes the instantaneous distribution of the mode frequencies among molecules of the substance, and therefore, reflects somehow the instantaneous inhomogeneities in the material. The parameter $\gamma_G(T)$ has a substantial temperature dependence in the range $T_g<T<T_A$ (Fig. 4). Taking into account the above remark on the high-temperature limit of 0.5 cm^{-1} for γ_G, we conclude from Fig. 4 that T_A serves as a specific temperature below which the remarkably nonequivalent states for molecules appear on a snapshot. At $T>T_A$ molecules can be considered as essentially equivalent in an effective medium. T_A is interpreted in Fig. 3 as the transition from single-molecule to cooperative relaxation dynamics, and this has a counterpart in the appearance of the dynamics inhomogeneities in Fig. 4.

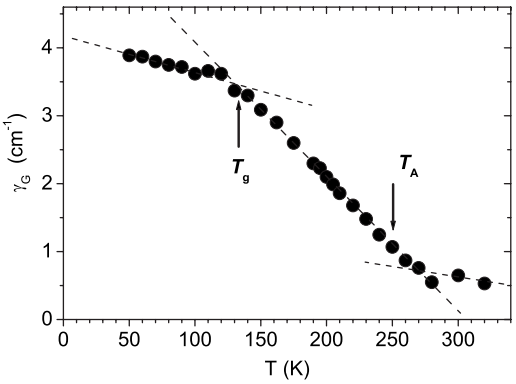

FIG. 4. Inhomogeneous broadening of the Raman line γ_G as extracted from Voigt's analysis, versus temperature. The dashed lines are guides for eyes.

The idea of a spatially heterogeneous relaxation response in supercooled liquids has now been recognized [17–20]. This idea was proven by experimental techniques with studying the relaxation response near T_g and by computer simulation at higher temperatures (e.g., Ref. [23]). The Raman line shape analysis allows one to consider another aspect of this problem and to visualize the inhomogeneity as a counterpart in the instantaneous distribution of the mode frequency. While the homogeneous-inhomogeneous transition, seen in Fig. 4, is rather in line with the modern models and computer simulations (e.g., Refs. [24,25]), there are no experimental techniques, revealing this transition. Figure 4 demonstrates that the Raman shape analysis offers an excellent capability for this goal, that this transition occurs at $T=T_A$, and that the transition is unexpectedly sharp.

In conclusion, the Raman line shape analysis in the molecular glass former α picoline is presented. Two striking outcomes are found. First, the orientational time, corresponding to rotational broadening, has an Arrhenius-like temperature dependence, even in the temperature range below T_A, where the α-relaxation time has a super-Arrhenius temperature dependence. Second, in the liquid state, the inhomogeneous broadening width almost linearly decreases as the temperature increases, marking a sharp transition at $T=T_A$. These results are interpreted to evidence a rather sharp transition from single-molecule to cooperative dynamics at $T=T_A$ during cooling and single-molecule-like relaxation of the orientational wavefunction at short times even at $T<T_A$.

This work was supported by RFBR Grant No. 06-03-32334, by the Interdisciplinary Science Fund of the Siberian Branch of RAS, and by the Russian Science Support Foundation.

[1] C. A. Angell, K. L. Ngai, G. B. McKenna, P. F. McMillan, and S. W. Martin, J. Appl. Phys. **88**, 3113 (2000).
[2] K. L. Ngai, J. Non-Cryst. Solids **275**, 7 (2000).
[3] P. G. Debenedetti and F. H. Stillinger, Nature (London) **410**, 259 (2001).
[4] S. P. Das, Rev. Mod. Phys. **76**, 785 (2004).
[5] F. J. Bartoli and T. A. Litovitz, J. Chem. Phys. **56**, 404 (1972).
[6] S. V. Adichtchev, St. Benkhof, T. Blochowicz, V. N. Novikov, E. Rössler, Ch. Tschirwitz, and J. Wiedersich, Phys. Rev. Lett. **88**, 055703 (2002).
[7] V. I. Berezin and M. D. El'kin, Russ. Phys. J. **15**, 1816 (1972).
[8] Ch. Tschirwitz and C. Alba-Simionesco, unpublished data taken from S. V. Adichtchev, Ph.D. dissertation, Bayreuth University, 2006.
[9] F. Stickel, E. W. Fischer, and R. Richert, J. Chem. Phys. **104**, 2043 (1996).
[10] C. A. Angell, J. Phys.: Condens. Matter **12**, 6463 (2000).
[11] F. Kremer, J. Non-Cryst. Solids **305**, 1 (2002).
[12] T. Blochowicz and E. A. Rössler, Phys. Rev. Lett. **92**, 225701 (2004).
[13] M. T. Cicerone and M. D. Ediger, J. Chem. Phys. **104**, 7210 (1996).
[14] L. Andreozzi, M. Faetti, and M. Giordano, J. Non-Cryst. Solids **352**, 3829 (2006).
[15] E. Rössler, Phys. Rev. Lett. **65**, 1595 (1990).
[16] F. Fujara, B. Geil, H. Sillescu, and G. Fleischer, Z. Phys. B: Condens. Matter **88**, 195 (1992).
[17] M. D. Ediger, Annu. Rev. Phys. Chem. **51**, 99 (1999).
[18] H. Sillescu, J. Non-Cryst. Solids **243**, 81 (1999).
[19] S. Glotzer, J. Non-Cryst. Solids **274**, 342 (2000).
[20] R. Richert, J. Phys.: Condens. Matter **14**, R703 (2002).
[21] V. K. de Souza and D. J. Wales, Phys. Rev. Lett. **96**, 057802 (2006).
[22] W. Kob and H. C. Andersen, Phys. Rev. Lett. **73**, 1376 (1994).
[23] G. S. Matharoo, M. S. Gulam Razul, and P. H. Poole, Phys. Rev. E **74**, 050502(R) (2006).
[24] L. Berthier and J. P. Garrahan, Phys. Rev. E **68**, 041201 (2003).
[25] C. Pareige, H. Zapolsky, and A. G. Khachaturyan, Phys. Rev. B **75**, 054102 (2007).